Title
Hyperpolarization moves S4 sensors inward to open MVP, a methanococcal voltage-gated potassium channel

Journal
Nature Neuroscience, 6(4)

ISSN
1097-6256

Authors
Sesti, Federico
Rajan, Sindhu
Gonzalez-Colaso, Rosana
et al.

Publication Date
2003-04-01

DOI
10.1038/nn1028

Hyperpolarization moves S4 sensors inward to open MVP, a methanococcal voltage-gated potassium channel

Federico Sesti[1,2], Sindhu Rajan[1], Rosana Gonzalez-Colaso[1], Natalia Nikolaeva[1] and Steve A.N. Goldstein[1]

[1] Departments of Pediatrics and Cellular and Molecular Physiology, Yale University School of Medicine, Boyer Center for Molecular Medicine, 295 Congress Avenue, New Haven, Connecticut 06536, USA

[2] Present address: UMDNJ-Robert Wood Johnson Medical School, Department of Physiology and Biophysics, 675 Hoes Lane, Piscataway, New Jersey 08854, USA

Correspondence should be addressed to S.A.N.G. (steve.goldstein@yale.edu)

Published online 17 March 2003; doi:10.1038/nn1028

MVP, a Methanococcus jannaschii voltage-gated potassium channel, was cloned and shown to operate in eukaryotic and prokaryotic cells. Like pacemaker channels, MVP opens on hyperpolarization using S4 voltage sensors like those in classical channels activated by depolarization. The MVP S4 span resembles classical sensors in sequence, charge, topology and movement, traveling inward on hyperpolarization and outward on depolarization (via canaliculi in the protein that bring the extra-cellular and internal solutions into proximity across a short barrier). Thus, MVP opens with sensors inward indicating a reversal of S4 position and pore state compared to classical channels. Homologous channels in mammals and plants are expected to function similarly.

Archeons have the cytological appearance of prokaryotes but significant homology to eukaryotes at the molecular level1. Members of this third domain of life were first noted for their capacity to thrive at extremes of temperature, pressure, pH and salinity. Their study has influenced theories of adaptation, yielded thermostable enzymes beneficial to basic and applied biotechnology and, owing to the relative ease of crystallization of thermophilic proteins, provided a wealth of structural information relevant to normothermic biology. M. jannaschii, isolated from a deep marine hydrothermal vent, is an obligate anaerobe that produces methane, grows optimally at pH 6 and 85˚C and provided the first archeal genome to be completely sequenced[2]. Among its 1,738 predicted products is MJ0139, which bears the hallmark of a protein that controls excitation of nerves and muscles in eukaryotes: voltage-activated potassium (K_v) channels.

K_v channel subunits have six transmembrane domains (S1–S6), including a charge-bearing fourth span (S4) and a pore-lining (P) loop between S5 and S6 that determines ion selectivity (Fig. 1a). Four K_v subunits almost certainly form a single, central ion conduction pore (Fig. 1b) like those in crystal structures of KcsA and MthK, bacterial and archeal channels with subunits comparable to the S5–P–S6 portions of K_v subunits[3,4]. Similarly, in voltage-gated sodium (Na_v) and calcium (Ca_v) channels, four K_v-like domains (linked together into one large subunit in eukaryotes but separate in a bacterial isolate[5]) form each pore.

Studies of classical Na_v and K_v channels that produce action potentials have rendered a detailed model for how changes in voltage are registered[6–16]: positive charges in the S4 spans (acting in concert with counter-charges in S2 and S3) serve as sensors. When the cell interior becomes more positive (depolarized), the S4 spans move outward (Fig. 1c), and gates that control ion flow through the pore open by an unknown mechanism. On returning to negative resting potentials, the S4 moves inward, and pore gates close. Movement of S4 charges is rapid because they traverse only a short barrier in the protein to enter spaces continuous with the external or internal solutions (Fig. 1c).

Pacemaker channels control action potential frequency and are activated by negative shifts in potential (hyperpolarization). It was recently discovered that pacemaker channels in the heart, brain and retina (HCN1–HCN4)[17–19] are also formed by K_v-like subunits (Fig. 1a). Six channels of this type are known in plants, including the KAT1 channel[20]. How classical and pacemaker channels respond to voltage stimuli of opposite polarity is an area of ongoing study[21–25].

In the present study, we show that the MJ0139 open reading frame encodes a Methanococcal, voltage-gated, potassium-selective channel (MVP) opened by hyperpolarization. MVP operated in both eukaryotes and prokaryotes, conferring survival to Saccharomyces cerevisiae and Escherichia coli cells deficient in potassium transport. The channels showed hyperpolarization-dependent latencies to first opening, half-maximal activation at –175 mV, and no prior requirement for depolarization, and they did not inactivate. The S4 span was shown to be oriented as in classical K_v subunits by an antibody binding assay. Sentinel cysteines introduced across the MVP S4 span showed side and voltage-dependent modification similar to that observed with depolarization-activated K_v channels. In both, S4 sites moved across a short barrier separating water-filled crevices in the

protein continuous with bulk solution. In contrast, inward S4 movements that close classical depolarization-activated channels opened MVP.

RESULTS

MJ0139 allows survival of transport-deficient cells

The M. jannaschii open reading frame for MJ0139 encodes a 209- residue predicted product with six probable transmembrane domains, a pore loop with a typical potassium channel signature sequence and an S4 span with multiple positively-charged residues arrayed as in other channels activated by voltage (Fig. 1d and e).

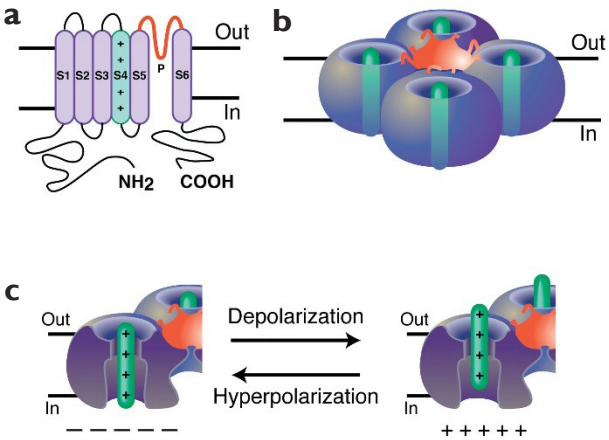

d

```
1.........10.........20.........
MNLKDRRLKKIMEVLSLIFTFEIVASFILST
                S1
YNPPYQDLLIKLDYISIMFFTFEFIYNFYYV
                S2
EDKAKFFKDIYNIVDAIVVIAFLLYSLQVFY
                S3
SKAFLGLRVINLLRILVLLRIIKLRKLEENQ
                S4
ALINFLTLLTICFIASCLIWIVESGVNPAIN
                S5
NFFDAFYFTTISITTVGYGDITPKTDAGKLI
                P
IIFSVLFFISGLITSLQKALKGD
                S6
```

e

```
          ..1..2..3..4..5..6..7.
Shaker    ILRVIRLVRVFRIFKLSRHSKG
S4/D4     LFRVIRLARIGRILRLIRGAKG
KAT1      GFRILSMLRLWRLRRVSSLFAR
HCN2      VYKTARALRIVRFTKILSLLRL
MVP       GLRVINLLRILVLLRIIKLRKL
```

Fig. 1. Amino acid sequence and predicted topology of MVP. (a) K_v sub- units contain six transmembrane domains (S1–S6), a voltage sensing fourth span (S4) with multiple positively-charged residues, and a pore (P) loop. (b) Four K_v subunits probably form a single, central ion conduction pathway. (c) A cut-away view suggesting how S4 sites that are intracellular at negative potentials (– – –) move outward on depolarization (+ + +)[9,12]: S4 crosses a short barrier between crevices in continuity with external or internal solution. In classical channels, depolarization-induced outward S4 movement opens the pore. (d) Predicted transmembrane spans for MVP (S1–S6, underlined) and pore loop (P, double underlined) based on free energy of transfer to water (window of 20 amino acids) and alignment to related proteins; potassium channel 'signature sequence' and positively-charged S4 residues are in bold. (e) Alignment of the S4 span in MVP (Acc. AAB98122) and the S4 in a depolarization-activated potassium channel, Shaker (Acc. JH0193), the fourth- domain S4 span (D4/S4) in a depolarization-activated sodium channel (Acc. M77235), and two hyperpolarization-activated channels: HCN2 (Acc. NP-001185) and KAT1 (Acc. S32816).

As the organism's natural environment presented significant experimental hurdles, we studied both the native gene and a synthetic version in cells more amenable to biochemical and biophysical studies. The synthetic gene was assembled de novo from six oligonucleotide pairs that maintain the native amino acid sequence while altering 62 of the 209 archeal codons to remove triplets inefficiently or ambiguously translated in first and second kingdom cells.

The MJ0139 product was first shown to function by its capacity to rescue CY162C S. cerevisiae cells that do not grow in low potassium media due to deletion of the genes for two potassium transporter proteins, TRK1 and TRK2[20]. While an empty plasmid vector was unhelpful to the cells, expression of either native or synthetic MJ0139 behind a constitutive ADH promotor supported cell growth on plates with 1 mM potassium (Fig. 2a, CY162C). Both the native and synthetic versions also conferred survival to TK2299 E. coli cells (Fig. 2a, TK2299) that otherwise did not grow when potassium levels were low because of disruption of the potassium transporter genes Kup, TrkG and TrkH[26].

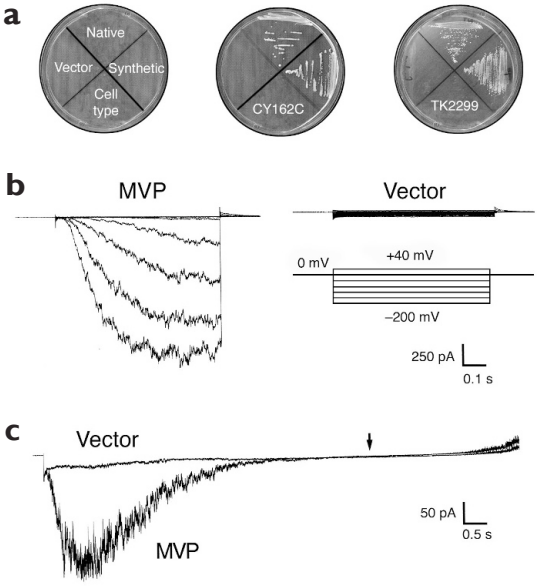

Fig. 2. MVP rescues yeast and bacterial cells and yields potassium currents. (a) CY162C yeast cells are unable to grow on plates with 1 mM potassium when they carry an empty plasmid (vector), but thrive with MJ0139 in native or synthetic form in the vector. TK2299 bacterial cells are unable to grow on 5 mM potassium plates with the empty plasmid (vector) but thrive with MJ0139 in native or synthetic form. (b) Whole- cell current in yeast cells expressing the native MVP gene or empty vector. Voltage protocol (inset): holding voltage 0 mV, 1-s steps from –200 to +40 mV in 20-mV increments; IPI, 2 s. (c) Whole-cell current in yeast cells expressing the native MVP gene or empty vector. Voltage protocol: a step from a holding voltage of 0 mV to –200 with linear ramp to +40 mV over 10 s. Scale bars are 50 pA, 0.5 s; arrow at 0 mV. Current in the positive voltage range is the endogenous, outwardly rectifying potassium channel TOK1 (ref. 28).

MVP passes potassium upon hyperpolarization

Yeast cells expressing MJ0139 showed a new voltage-gated, potassium-selective ion channel opened by hyperpolarization (MVP). Removal of the cell wall to produce spheroplasts allowed measurement of plasma membrane currents in whole-cell and patch modes, as done previously[27,28]. With steps to negative potentials, MVP currents activated after a delay and did not inactivate (Fig. 2b, left); in contrast, control cells carrying empty vector were almost silent in this voltage range (Fig. 2b, right). As expected, small outward currents carried by the potassium channel native to yeast cells (TOK1) were apparent on depolarization with both cell types (Fig. 2c, right of arrow)[27–29].

Macroscopic MVP currents showed half-maximal activation ($V_{1/2}$) at –175 ± 33 mV with a slope factor (V_s) of 26 ± 4 mV yielding an apparent gating charge (z_0) of 1.1e (Fig. 3a). The time course for activation was voltage-sensitive and, after the delay, was well-fitted by a single exponential that decreased linearly with a slope of ~8 mV per ms (time constant, $\tau = 0.77 \pm 0.15$ at –140 mV) (Fig. 3b). Neither internal cAMP nor cGMP at 1 mM altered the activation midpoint, slope or kinetics (data not shown).

MVP channels were found to be selective for potassium, first by progressive substitution of bath

potassium with sodium; this decreased inward currents and shifted reversal potential by kT/e = 24 □ 1 mV (k, Boltzmann constant; T, temperature in degrees Kelvin; e, electronic charge) when fit to a Nernst equation under conditions predicting a value of 25.6 for ideal potassium selectivity (Fig. 3c). Selectivity among monovalent cations was assessed by bi-ionic permeability (P) ratios and corresponded to a type IV series: potassium > rubidium > cesium > sodium = lithium, with sodium ~100-fold less permeant than potassium ($P_{Na}/P_K \approx 0.01$)

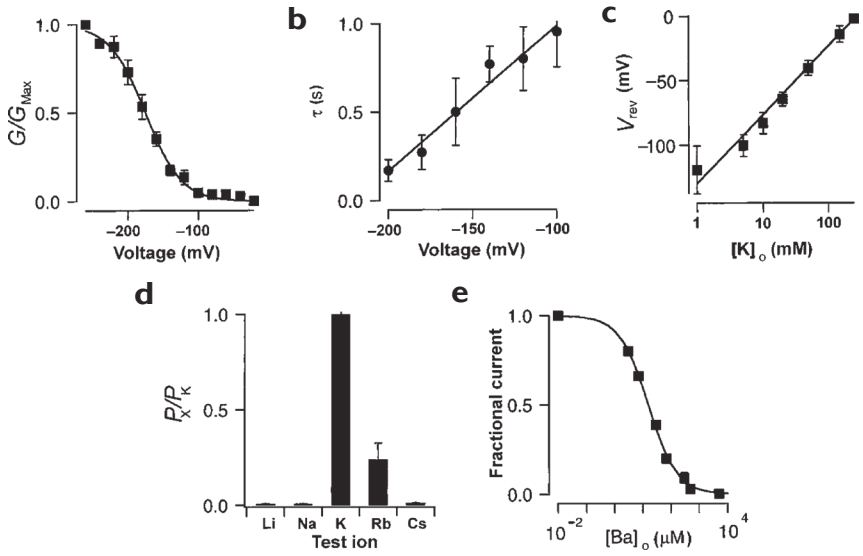

Fig. 3. MVP currents: activation and selectivity. MVP expressed from the native gene in CY162C yeast cells are characterized in these panels; currents from the synthetic gene were indistinguishable in magnitude, $V_{1/2}$, V_s, kinetics, selectivity and blockade (n = 3–8 cells). (a) Steady-state activation of MVP by hyperpolarization; normalized conductances (G/Gmax) calculated from macroscopic currents. Based on roughly equal potassium levels across the membrane $E_K = 0$ mV was assumed and data fitted to a Boltzmann function: $1/\{1 + \exp[(V_{1/2} - V)/V_s]\}$ giving $V_{1/2} = -175 \pm 33$ mV and $V_s = 25.6 \pm 4.0$ ($z_0 = 1.1e$). Data for eight cells to –200 mV and four cells to –260 mV. (b) Kinetics of MVP activation; activation time course fitted after a delay to a single exponential decreased linearly with a slope of 8.2 ± 0.8 ms per mV. Data from five cells. (c) MVP is selective for potassium over sodium; peak tail reversal potential was measured with various external potassium levels by isotonic substitution with sodium. Data fit to a Nernst function:

$$E_K = \frac{kT}{e} \ln \frac{[K]_o}{[K]_i}$$

where k is the Boltzmann constant, T the temperature in Kelvin and e is electronic charge; perfect selectivity gives kT/e ≈ 25.6 mV versus 24 ± 1 mV from a fit to the data. Data were calculated from current envelopes by isotonic replacement for sodium with holding voltage 0 mV, 1 s pre-pulse to –200 mV followed by 2-s steps from –200 mV to +40 mV; IPI, 2 s. Data from four cells. (d) MVP is most permeable to potassium among monovalent cations tested; permeability ratios were computed according to: $P_x/P_K = \exp(eE_{rev}/kT)$ where E_{rev} is the reversal potential as determined from peak tail reversal as in (c). Test cations replacing potassium (K) in the bath were rubidium (Rb), cesium (Cs), sodium (Na) and lithium (Li). Data from 4 cells. (e) Barium blocked MVP currents from the external solution in a voltage-dependent manner. Panel shows dependence of fractional current (I/Io) with increasing bath barium at –200 mV for groups of five cells, half-block (K_i) of 17 ± 2 μM. Voltage dependence of block assumed a bimolecular interaction and energy profile of two barriers and one well with the internal barrier infinitely high so that blocked current was:

$$\frac{I}{I_{max}} = I_{min} + I_o \exp\left[\frac{z(1-\delta)eV}{kT}\right]$$

where z is the charge of the blocker, I_{min} the current for $V \to \infty$ and I_o related to the voltage-independent part of the profile. δ is the apparent electrical distance and represents the fraction of the voltage drop experienced by the blocker, and was determined to be 0.20 ± 0.07.

(Fig. 3d). MVP currents were blocked by the classical potassium channel inhibitor barium in a voltage-dependent manner such that 17 μM in the bath blocked half the current at –200 mV with an apparent electrical distance (δ) of 0.2 (Fig. 3e).

Hyperpolarization opens single MVP channels

Single MVP channels were readily identified in yeast cell membrane patches by their characteristic activity at negative potentials (Fig. 4a) and potassium selectivity (Fig. 4b). No similar channel was observed in 40 control cells. Evaluated from –100 to –200 mV, single-channel slope conductance was $\gamma_s = 37 \pm 7$ pS (Fig. 4c). Single-channel recordings showed that hyperpolarization increased MVP activity via an increase in open probability in a manner well-fitted to the curve for macroscopic current activation with the same $V_{1/2}$ and V_s values (Figs. 3a and 4d). Single-channel gating kinetics were best described by a single open dwell time and

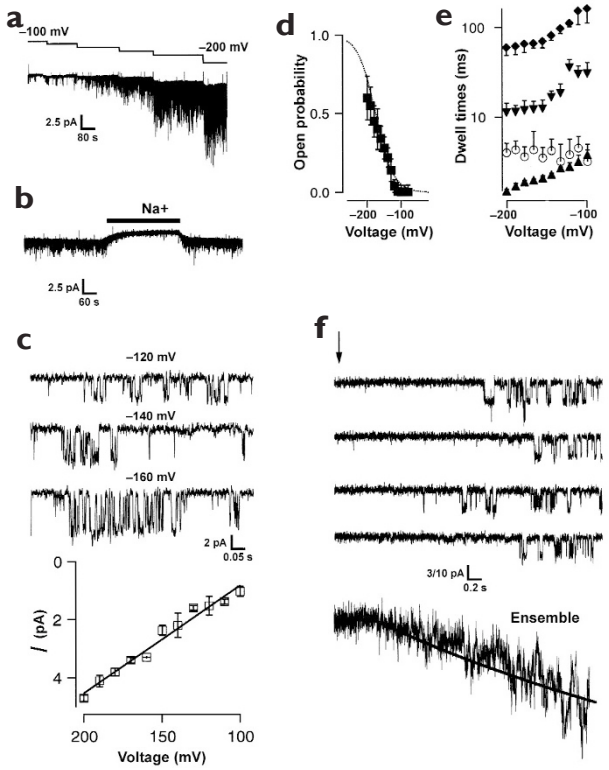

Fig. 4. Single MVP channels are opened by hyperpolarization. CY162C yeast cells expressing the synthetic MVP gene are characterized here; channels from the native gene had the same attributes (2–4 cells). (a) Single-channel activity in an outside-out patch with three MVP channels held at –100 mV and stepped to indicated voltages. For display data filtered to 100 Hz and sampled at 500 Hz. (b) Replacement of bath potassium with sodium reversibly suppressed MVP unitary currents. Mode as in (a) (–140 mV) with a change from 150 mM potassium to 150 mM sodium in the bath (bar). Scale bars are 3 pA and 100 s. (c) Representative single- channel trace at three indicated voltages and I–V relationships from six patches. For display data was filtered at 500 Hz and sampled at 2 kHz. A linear fit gives slope conductance, $\gamma = 37 \pm 7$ pS. (d) Voltage-dependence of the mean open probability. The dashed line corresponds to the fit of the G/G_{max} curves from macroscopic currents (Fig. 3a). For analysis, data were filtered to 2 kHz and sampled at 6 kHz, and a half-amplitude threshold method was applied. Data from three patches. (e) Voltage-dependence of open and closed dwell times. Data filtered to 2 kHz, sampled at 6 kHz and plotted on a logarithmic scale with a square-root vertical axis to best discern event populations and fitting to compensate for missed events, as before[28]. Unfilled symbols are open times; filled symbols are closed times. Dead time, -100 μs; from three patches. (f) Representative latencies to first opening on steps to –160 mV from 0 mV (with IPI of 2 s) showing the average of 98 sweeps (ensemble); the delay and exponential fall of the ensemble was well-fitted by the time course for development of whole-cell currents at –160 mV ($\tau = 0.47 \pm 0.12$ s; Fig. 3b). A histogram of the latencies fit after a delay to a single exponential gave $\tau =$ 143 ± 8 ms with a peak at 200 ms

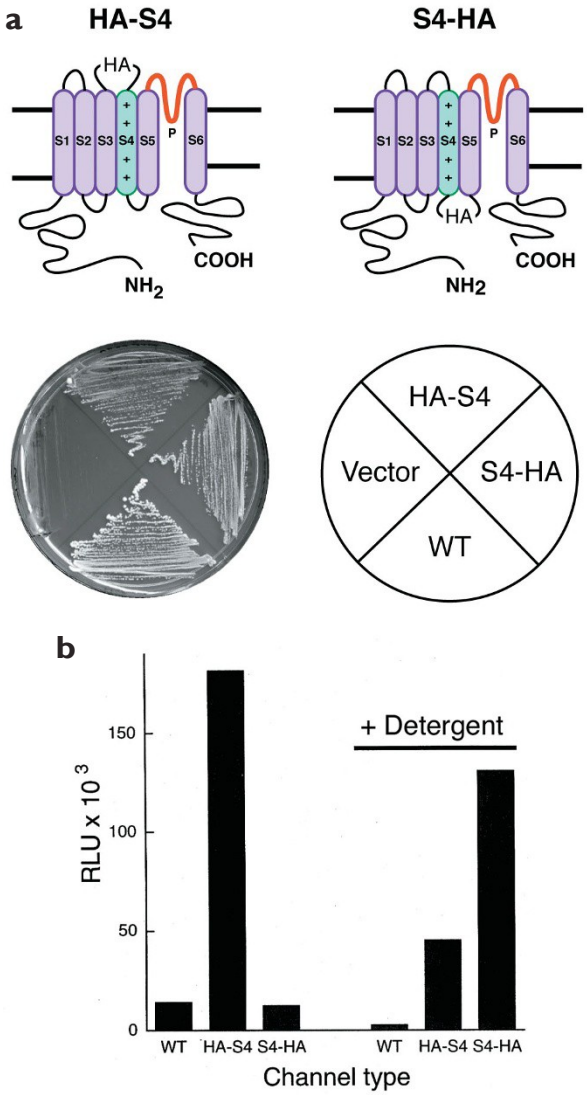

Fig. 5. The MVP S4 is upright in the membrane. CY162C yeast cells expressing the wild type (WT) synthetic MVP gene and two variants. Drawings of predicted topologies of MVP channels with HA tag introduced before (HA–S4) or after (S4–HA) the S4 span. Photograph shows growth of cells expressing the variant channels on 1 mM potassium plates indicating both were functional. (b) Surface expression of HA-tagged MVP channels was quantified by antibody binding and luminometry. Whereas untagged wild-type MVP (WT) and S4–HA channels showed background readings, HA–S4 channels yielded a strong surface signal supporting external exposure of the tag. After detergent exposure (+ detergent), antibody could enter the cell, and S4–HA channels also showed a strong signal. Plot is raw relative light units (RLU) for groups of 10^7 cells, minus the nonspecific signal of cells expressing WT MVP processed without antibody to HA.

three closed times (τ_o = 3.2 ± 0.8 ms, τ_{C1} = 2.7 ± 0.1 ms, τ_{C2} = 18.6 ± 5.1 ms and τ_{C3} = 98 ± 12 ms at –140 mV, Fig. 4e). Whereas open times were fairly stable to changes in voltage, closed times shortened modestly at more positive potentials, suggesting that hyperpolarization increased the frequency rather than duration of open events. Latencies to first opening showed a delay and exponential rise, as observed with macroscopic currents (Fig. 4f) and no requirement for prior depolarization (null frequency 2/100).

Studies of single MVP channels in TK2299 bacterial cells proved feasible after suppression of mitosis and removal of the cell wall to produce multi-nucleated tube structures by a described method[30], although stable patches were difficult to obtain. Single channels from the synthetic gene in two long-lasting patches showed the same apparent slope conductance (γ_s = 38 ± 6 pS) and gating kinetics as in yeast cells (τ_o = 3 ± 1, τ_{C1} = 4.2 ± 1.1, τ_{C2} = 16.1 ± 4 and τ_{C3} = 109 ± 19 ms, –140 mV), supporting the idea that MVP operated similarly in prokaryotic and eukaryotic cells.

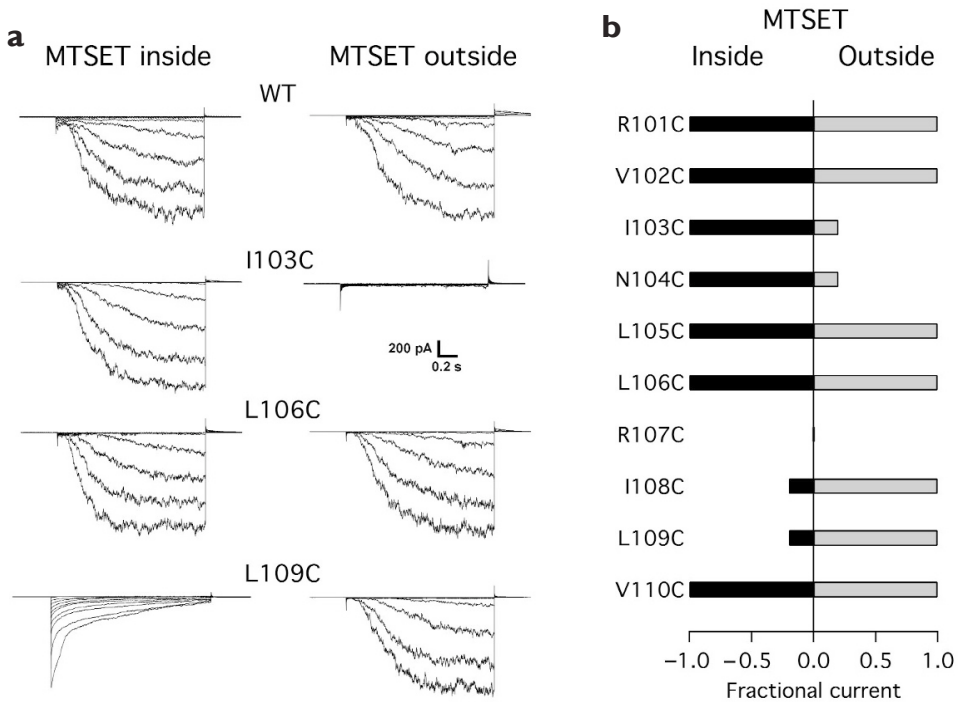

Fig. 6. Modification of sentinel cysteines in S4 is side and voltage-dependent. CY162C cells expressing wild type synthetic MVP and nine mutant channels with a single S4 residue altered to cysteine studied in whole-cell mode with 5 mM MTSET in the internal or external solution. R107C-MVP did not yield currents. (a) Representative current traces from cells expressing wild-type MVP (WT) or the indicated channel mutant with MTSET inside or outside. Protocol: holding 0 mV, 1-s steps from –200 to +40 mV in 20-mV increments; IPI, 2 s. Scale bars represent 600 pA and 0.2 s for L109C with internal MTSET. (b) Fractional current after exposure to MTSET from the inside or outside measured at the end of a 1 s step to –200 mV (after repetition of the protocol in (a) for 5–10 min). Wild-type MVP and five variants (R101C, V102C, L105C, L106C and V110C) were not altered by MTSET from either side of the membrane. External MTSET inhibited I103C and N104C channels, and internal MTSET altered I108C and L109C channel function. Data for 3–5 cells ± s.e.m.

S4 orientation: MVP and classical channels are the same

To assess membrane orientation, we introduced an eight-residue tag from hemagglutinin (HA) before the S4 segment of MVP (HA–S4) or after the span (S4–HA) and studied the tagged channels in yeast cells (Fig. 5a). To confirm that the tags did not significantly disrupt structure, both new channels were shown to retain the capacity to rescue CY162C yeast cells on low-potassium medium (Fig. 5a), indicating that the inserts neither interfered with surface expression nor markedly disrupted function. Exposure of the tag was assessed with anti-HA antibodies and yeast spheroplasts that were intact or detergent-treated to allow access to the spheroplast interior; a secondary antibody conjugated to horseradish peroxidase was then applied in a variation of a luminometry method previously developed for Xenopus laevis oocytes31.

The MVP S4 span was found to be oriented as in classical channels. With intact cells, channels with the tag after the S4 span (S4–HA) yielded the same null fluorescence as did cells with untagged wild-type MVP (WT), whereas HA–S4 channels yielded a strong signal consistent with external exposure of their tag (Fig. 5b). Conversely, S4–HA channels gave a strong signal when pretreatment with detergent allowed antibodies to pass through the plasma membrane, supporting an internal location for the tag when it followed the S4 span (Fig. 5b).

Side-dependent modification of MVP S4 sites

Classical K_v channels carry four S4 spans that move outward on depolarization and inward on hyperpolarization, past a short barrier in the protein separating spaces that communicate with the external or internal solutions (Fig. 1c and e)[12,13]. To assess the behavior of S4 sites in MVP, we used a cysteine-scanning/covalent modification approach. Exposure was examined with methanethiosulfonate

tetraethylammonium (MTSET), a positively-charged, water-soluble, membrane-impermeant agent that reacts with free sulfhydryls. Ten MVP channels were produced with a single S4 residue altered to cysteine (R101 to L110). Nine of the variants supported growth of CY162C cells in low potassium (data not shown) and passed currents similar to wild type (Fig. 6a); R107C subunits did neither and were not studied further.

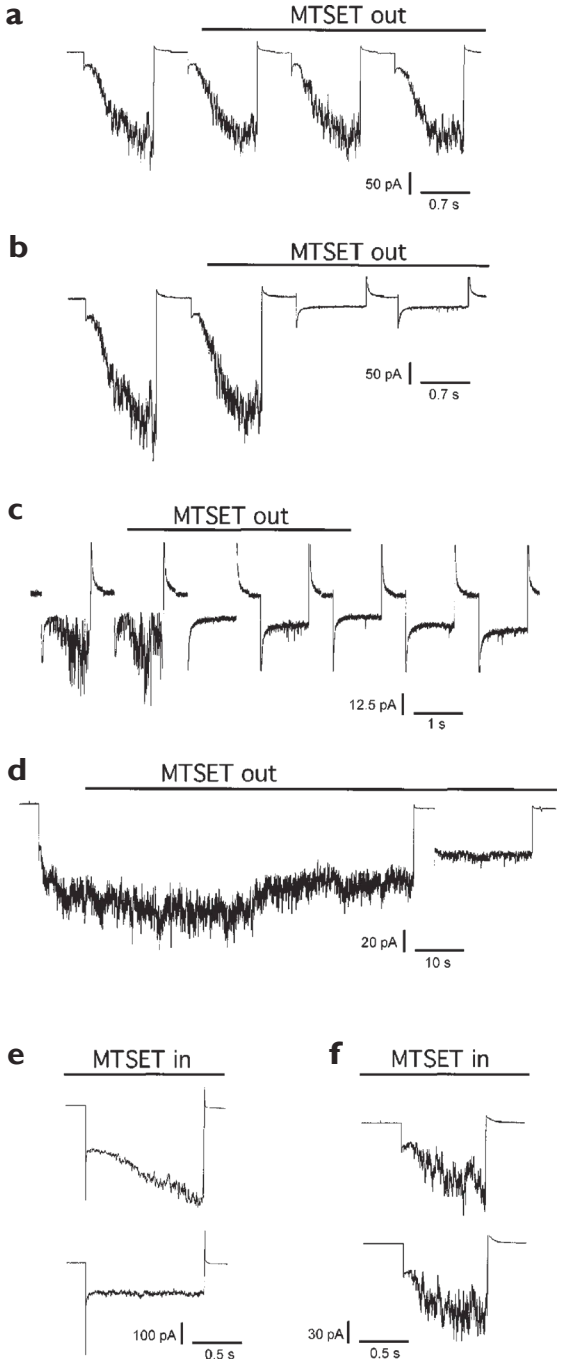

Fig. 7. Modification of sentinel cysteines in S4 is state-dependent. CY162C yeast cells expressing MVP channels were studied in whole-cell mode with 5 mM MTSET applied from outside (bars) or in the pipette. Protocol (a–c): repetitive 1-s steps from 0 to –200 mV with a 0.5-s IPI. Wild-type MVP channels were insensitive to external MTSET. N104C MVP channels were inhibited by external MTSET only after a step to 0 mV closing the channels (between epochs 2 and 3). (c) I103C MVP channels were inhibited by external MTSET only after a step to 0 mV closing the channels (between epochs 2 and 3). (d) N104C MVP channels were protected from 65 s exposure to external MTSET at –140 mV (open channels) but blocked by a 5-s step at 0 mV. (e) L108C MVP channels were protected from internal MTSET (whole-cell mode, reagent in pipette) at a holding voltage of 0 mV; this was revealed by 1-s test step to –200 mV taken after 5 min at 0 mV in whole cell configuration (top); the next test pulse (3 s later) shows that channels were modified as a result of the first stimulatory test hyperpolarization (bottom). (f) N104C MVP channels were insensitive to internal MTSET (whole-cell mode, reagent in pipette) whether it was the first 1-s test step to –200 mV taken from a holding voltage of 0 mV (top) or subsequent cycles (bottom, 4th repeat shown).

Application of MTSET from either face of the membrane for 5–10 minutes with repetitive voltage steps from +40 to –200 mV had no effect on wild-type MVP channels; this indicated that the two natural cysteines were either unmodified or that their modification did not alter function (Fig. 6a and b). This was not true of four channels with an introduced cysteine. As rapidly as external MTSET was added to the recording chamber, activity of I103C and N104C channels was suppressed, whereas internal reagent (in the pipette) had no effect. Reciprocally, internal MTSET altered the gating kinetics of I108C or L109C channels as soon as pulse stimuli were applied (to yield rapidly activating and inactivating currents), whereas reagent applied externally had no effect (Fig. 6a and b). Five MVP variants (R101C, V102C, L105C, L106C and V110C) were unaltered by MTSET from either side of the membrane (Fig. 6a and b). Side-dependent reactivity of these sites supported the conclusion drawn from antibody binding studies (Fig. 5b) that S4 spans in MVP and classical channels have the same orientation in the membrane. That internal MTSET did not alter function of N104C channels, and external MTSET did not influence I108C channels, indicated that neither site was exposed to reagent on the opposite side of the membrane (Fig. 6b).

S4 moves inward on hyperpolarization

The effects of 5 mM MTSET on susceptible mutants depended not only on the side of reagent application but also on applied voltage/channel state. Thus, external MTSET had no effect on wild-type MVP channels whether open or closed (Fig. 7a) or N104C channels if applied during an opening step to –200 mV (Fig. 7b, epoch 2); however, closing N104C channels by depolarization to 0 mV for just 0.5 s (Fig. 7b, between epochs 2 and 3) led to complete current suppression, as seen on a subsequent step to –200 mV (Fig. 7b, epoch 3). Reaction of external MTSET with I103C channels was also limited to the closed state (Fig. 7c); moreover, as expected for covalent modification by the reagent, inhibition was not reversed on MTSET wash-out with I103C (Fig. 7c) or N104C channels (data not shown). Also consistent with hyperpolarization-induced inward movement of N104C and external exposure of the site on depolarization, the site was protected from bath MTSET for 65 s at –140 mV, but suppressed after a depolarizing step to 0 mV (Fig. 7d). Because inside-out patches from yeast cells expressing MVP cysteine mutants passed small currents, state-dependent internal exposure was assessed qualitatively in whole-cell mode as follows: with MTSET in the pipette, depolarization was maintained after achieving whole cell mode, and after a delay, the effects of hyperpolarization were studied. Thus I108C channels were protected from internal MTSET for 5 minutes by depolarization to 0 mV, as revealed by a step to –180 mV (Fig. 7e, top), but modified after hyperpolarization (Fig. 7e, bottom). Conversely, N104C channels remained insensitive to internal reagent despite hyperpolarization (Fig. 7f).

Overall, the findings support outward displacement of S4 on depolarization, inward movement on hyperpolarization, and a barrier that protects three S4 residues from MTSET.

DISCUSSION

MVP is an archeal potassium channel activated by hyperpolarization. Encoded by M. jannaschii, the channel operates in bacterial and yeast cells, arguing for shared mechanisms of transport in the three life domains. To explore the basis for activation of MVP channels, we examined their functional attributes, the orientation of their S4 spans and the side and voltage-dependent exposure of sites across the S4 segments. Four explanations for activation by hyperpolarization seem plausible. First, the channels might be ‘upside-down’ in the membrane, similar to GluR0, a glutamate receptor[32]. Second, depolarization might open the channel but lead to rapid inactivation so that significant currents flow only after recovery from inactivation upon hyperpolarization, as for HERG potassium channels[33,34]. Third, hyperpolarization might act elsewhere on the protein to release S4 from an energetically unfavorable inward locale, allowing it to move outward to open the pore. And fourth, hyperpolarization might move S4 inward to open the channel, indicating a reversal of the coupling between sensor position and pore state compared to classical channels activated by depolarization. This report best supports the last explanation. We did not find an inverted orientation of the MVP S4 spans (Fig. 5). MVP showed hyperpolarization- dependent latencies to first opening, half-maximal activation at –175 mV with a shallow voltage-dependence ($z_0 \approx 1.1e$), no requirement for prior depolarization and no inactivation on hyperpolarization (Figs. 2–4); these findings argue against a HERG-like mechanism but do not

rule it out. Finally, on the basis of residue accessibility to covalent modification, we conclude that hyperpolarization moved the MVP S4 span inward, not outward (Figs. 6 and 7). It follows that if the S4 spans in MVP and classical channels are similarly oriented and alter their location with the same polarity on changes in voltage, the relationship between S4 position and pore state in the two channel types must be reciprocal; that is, MVP opens when the S4 spans move inward, whereas classical channels close.

Similar S4 canaliculi in classical and MVP channels

When cysteines are introduced into the fourth S4 span of a voltage-gated sodium channel and probed with the same large (6–8 Å) thiol reagent used here, the second and third positively charged sites move completely from internal to external exposure (Fig. 1e, D4/S4, R2C and R3C)[9,10]. Moreover, R3C is accessible from outside in the open state, whereas R4C (just 3 sites away) is exposed internally. As the distance between these sites could be as small as 4.5 Å (if α-helical) or up to 11 Å if extended, the S4 span is thought to reside in a water-filled canal (large enough to accommodate the modifying reagent) and moves relative to a barrier much shorter than the ~40 Å plasma membrane bilayer. The same approach has been used with Shaker channels, providing evidence for an S4 canal with a short barrier that allows external access to R1C, simultaneous with internal exposure of R3C and protection of up to five residues from the reagent (Fig. 1e)[12]. Elegant support for a water-filled canal with a short barrier in Shaker channels also comes from a study in which histidine residues were introduced into the S4; this allowed shuttling of protons across the membrane, indicating movement of R2H, R3H and R4H completely from the intracellular compartment in the closed state to a space continuous with external solution on channel opening. Thus, as judged by the smaller proton probe, the barrier appears to be quite short since steady proton currents are seen at some voltages[13,16].

Our data suggest that MVP S4 spans undergo voltage- dependent movements like those observed in classical K_v channels. Thus, hyperpolarization protected cysteines in MVP at I103C and N104C from modification by external MTSET, consistent with inward movement of S4 (Fig. 7a–d). On depolarization, I103C and N104C were exposed to external reagent, whereas I108C was protected from internal MTSET, consistent with outward S4 movement and occlusion of three contiguous S4 sites from the reagent (Figs. 6 and 7). Thus, MVP was similar to Shaker as judged by MTSET in that no S4 site traveled completely across the barrier, and multiple S4 residues were simultaneously protected. That external modification of I103C and N104C stabilized the closed channel state suggests that the methanethio-sulfonate adduct interferes with inward S4 movement and channel opening (Figs. 6a and 7a–d). Conversely, modification of I108C (Fig. 7e) and L109C (Fig. 6a) from the inside led to rapid channel activation on hyperpolarization as if outward S4 movement, and thereby transition away from the open state, had become limited. These findings point to a direct correlation between an inward S4 locale and an open pore supporting the operation of MVP S4 segments as voltage sensors.

Comparison with other channels

Owing to their homologous sequences and gating behaviors, archeal, mammalian and plant pacemaker-type channels are expected to operate similarly. MVP and HCN channels are similar in their activation by hyperpolarization, but different in ion permeation and regulation. HCN channels are permeable to sodium ($P_{Na}/P_K \approx 0.2$) despite bearing canonical potassium channel pore signature sequences[35,36], whereas MVP is potassium- selective ($P_{Na}/P_K \approx 0.01$). The unitary conductance of HCN2 (data not shown) and native pacemaker channels[37] is estimated to be ~1–2 pS, whereas that for MVP is ~37 pS (Fig. 4). Exposure to cyclic nucleotides shifts the activation midpoint of HCN channels positively by 2–23 mV35, whereas MVP has no analogous binding domain or response. HCN and MVP channels are similar in voltage-dependence ($z_0 \approx 1e$) and activation kinetics ($\tau \approx 150$ ms at –140 mV), and whereas cloned HCN subunits activate more positively ($V_{1/2}$ roughly –75 to –100 mV), many native channels are like MVP ($V_{1/2}$ roughly –140 mV)[36].

Notably germane to the present study is a recent report on a sea urchin HCN channel (spHCN) probed at eight S4 positions by cysteine mutation and MTSET application[25]. The S4 spans in spHCN appear to respond to voltage as do those in classical voltage-gated channels, the same conclusion we draw here for MVP. Our work supports their assumption that S4 spans are oriented as in depolarization-activated channels[25]; reciprocally, our qualitative assessment of internal state-dependent exposure finds support in their analysis of MTSET

modification rates[25], studies that were not feasible in our system.

KAT1 and MVP are markedly different only in their regulation. They share a type IV selectivity series[20] and have comparable single-channel attributes[21]; KAT1 has a unitary conductance of ~8 pS, a single open dwell time ($\tau_o \approx 10$ ms) and two closed times ($\tau_{C1} \approx 4$ ms and $\tau_{C2} \approx 100$ ms); MVP shows a third closed state of intermediate duration (~10 ms) (Fig. 4e). KAT1 is active in the same voltage range ($V_{1/2} \approx -150$ mV) and shows similar activation kinetics ($\tau \approx 0.9$ ms at –140 mV) and equivalent gating charge ($z_0 \approx 1.4e$)[20,38,39]. In contrast, the $V_{1/2}$ of KAT1 activation shifts on cGMP exposure to more negative potentials[38]. HCN, KAT1 and MVP open more slowly and with weaker voltage- dependence than depolarization-activated K_v and Na_v channels, which yield $z_0 \approx 4.5e$ by the strategy applied here (direct assessment of gating currents or limiting slope of ionic conductances increase these values roughly 2–3 fold).

Coupling of S4 and pore gates

Depolarization of Shaker channels relaxes a restriction to ion flow at the intracellular end of the conduction pathway[40]; similarly, hyperpolarization relaxes the intracellular aspect of spHCN channels[24]. In each case, activation by a change in voltage allows ions in the cytoplasm to gain access to cysteine residues substituted at sites higher in the pore. In Shaker-type channels depolarization is also associated with changes at (and around) the ion selectivity filter[41–44]. How voltage-induced movements of S4 spans are coupled to an altered pore state remains to be elucidated.

It is notable that two other channel types that use P loops to form their pores (but do not contain charge-bearing S4 spans) apparently use related gating strategies. On ligand binding, cyclic nucleotide–gated channels do relax an internal pore restriction, but this area does not impede flux of permeant ions, which cross the membrane only after changes near the selectivity filter[45,46]. Gating of 2P-domain potassium leak (K2P) channels also involves changes in the outer aspect of the ion conduction pore like those seen in Shaker channels[47].

METHODS

Plasmids, synthesis of MVP and mutants. Native and synthetic MVP genes were expressed in yeast cells in a variant of pRS426 (Stratagene, La Jolla, California) bearing the ADH1 promotor and terminator. The genes were inserted into the BAMH1-SAC1 sites in pTRCHisA (Invitrogen, Carlsbad, California) for expression in TK2299 cells. The sequences of the six synthetic oligonucleotide pairs that were annealed and ligated into pTRCHisA to yield the synthetic MVP gene are cataloged with the final product under GenBank accession number AF508327. Point mutations were produced by PCR, and altered gene products were confirmed by automated DNA sequencing. HA tags encoding LAYPYDVPDALG were inserted by the same method into synthetic MVP replacing residues 97 and 98 in HA–S4–MVP and 124 and 125 in S4–HA–MVP.

Yeast and bacterial K^+ transport–deficient strains. CY162 cells (*MATa ura3-52 his3Δ200 his4-15 trk1Δ trk2Δ:HIS3*), a trk1, trk2 strain, were a gift from R. Gaber[48]; after the cells were cured of M1 virus by multiple rounds of growth at 40 ˚C on YPD plates, they were designated CY162C[28]. TK2299 *E. coli* cells (*F– thi rha* $lacZ_{am}$ *nagA endA Δ(kdpFAB)5 trkD1 trkA405*) were a gift from W. Epstein (Chicago)[26]; the trkD1 and trkA405 mutations abolish Kup and TrkG+TrkH transport function, respectively.

Media. Yeast and bacterial media and methods were conventional. For yeast cell transformation, we used 40% PEG 2000, 100 mM lithium acetate, TE with 10 μg boiled salmon sperm carrier DNA and selection on uracil-deficient plates. High and low potassium plates for CY162C cells were uracil-deficient and contained complete synthetic medium with 100 mM KCl or arginine phosphate dextrose with 1 mM KCl, respectively, as done previously[49]. High and low potassium media for TK2299 bacterial cells were standard LB-ampicillin with substitution of 100 or 5 mM KCl for NaCl.

Electrophysiology. Spheroplasts were produced and enriched by centrifugation through a sorbitol cushion for electrophysiology as before[28]. Data were recorded with an Axopatch 200B (Axon Instruments, Union City, California), a Quadra 800 Macintosh computer and Pulse software (Heka, Lambrecht, Germany) at filter and sampling frequencies of 0.5 kHz and 2.5 kHz, respectively, if not otherwise stated. Holding voltage was 0 mV with 1-s steps from –200 to +40 mV in 10 mV increments with an interpulse interval (IPI) of 2 s

unless noted otherwise. Pipette solution contained 175 mM KCl, 5 mM MgCl, 10 mM EGTA, 1 mM CaCl, 10 mM HEPES, pH 7.0 with KOH. Bath solution, unless otherwise indicated, was 150 mM KCl, 10 mM CaCl, 5 mM MgCl, 10 mM HEPES, pH 7.5 with KOH. Solid MTSET (Toronto Research Chemicals, North York, Ontario) was freshly dissolved in bath or pipette solution and used for 60 min. About 25% of control and MVP-expressing CY162C cells showed a stretch-activated cation channel distinguished by its unitary current and gating kinetics[50], and these were discarded.

Quantitative chemiluminescence. CY162C cells expressing wild-type and HA-tagged channels were collected at early logarithmic growth (OD_{600}, 0.7–1.0), incubated at 30 ˚C in 1 M sorbitol, 10 mM sodium citrate, 10 mM EDTA, 10 mM DTT and 100 µg/ml zymolase (20T, ICN) for 40 min. Spheroplasts were purified by centrifugation at 500g over a 1.5 M sucrose cushion to remove dead cells and cell-wall debris. To expose the internal tag, we treated spheroplasts with 0.1% Triton X-100 for 15 min in wash buffer: 250 mM KCl, 10 mM $CaCl_2$, 5 mM $MgCl_2$, 0.5% glucose and recovered by centrifugation at 500g. Aliquots of 10^7 sphero- plasts were incubated overnight at 4 ˚C in 1 ml wash buffer with 0.2% bovine serum albumin (BSA) and 5 µg/ml anti-HA mouse monoclonal antibody 12CA5 (Roche, Basel, Switzerland). At 4 ˚C, the spheroplasts were then washed four times (15 min) with wash buffer, incubated with goat anti-mouse HRP-labeled antibody at 1:20,000 dilution in wash buffer containing 0.2% BSA for 1 h, and then washed three times in wash buffer (the last time without BSA). Spheroplasts were resuspended in 1 ml SuperSignal ELISA Femto maximum sensitivity substrate (Pierce, Rockford, Illinois), incubated for 1 min after addition of 1 ml luminol/enhancer and studied in a LUMAT LB 9501 Luminometer (EG&G, Berthold, Bad Wildbad, Germany).

GenBank accession numbers: AF508327, AAB98122, JH0193, M77235, NP-001185, S32816.

Acknowledgments

This work was supported by grants to S.A.N.G. from the National Institutes of Health. S.A.N.G. is a Doris Duke Charitable Foundation Distinguished Clinical Scholar Award recipient. We thank R. Goldstein for technical and lexical support.

Competing interests statement

The authors declare that they have no competing financial interests.

RECEIVED 24 DECEMBER 2002; ACCEPTED 29 JANUARY 2003

1. Woese, C.R., Kandler, O. & Wheelis, M.L. Towards a natural system of organisms: proposal for the domains Archaea, Bacteria and Eucarya. *Proc. Natl. Acad. Sci.* USA **87**, 4576–4579 (1990).
2. Bult, C.J. et al. Complete genome sequence of the methanogenic archaeon, *Methanococcus jannaschii. Science* **273**, 1058–1073 (1996).
3. Zhou, M., Morais-Cabral, J.H., Mann, S. & MacKinnon, R. Potassium channel receptor site for the inactivation gate and quaternary amine inhibitors. *Nature* **411**, 657–661 (2001).
4. Jiang, Y.X. et al. Crystal structure and mechanism of a calcium-gated potassium channel. *Nature* **417**, 515–522 (2002).
5. Ren, D. et al. A prokaryotic voltage-gated sodium channel. *Science* **294**, 2372–2375 (2001).
6. Hodgkin, A.L. & Huxely, A.F. A quantitative description of membrane current and its application to conduction and excitation in nerve. *J. Physiol. (Lond.)* **117**, 500–544 (1952).
7. Sigworth, F.J. Voltage gating of ion channels. *Q. Rev. Biophys.* **27**, 1–40 (1994).
8. Hoshi, T., Zagotta, W.N. & Aldrich, R.W. Shaker potassium channel gating. I: Transitions near the open state. *J. Gen. Physiol.* **103**, 249–278 (1994).
9. Yang, N. & Horn, R. Evidence for voltage-dependent S4 movement in sodium channels. *Neuron* **15**, 213–218 (1995).
10. Yang, N., George, A.L. Jr. & Horn, R. Molecular basis of charge movement in voltage-

gated sodium channels. *Neuron* **16**, 113–122 (1996).
11. Seoh, S.A., Sigg, D., Papazian, D.M. & Bezanilla, F. Voltage-sensing residues in the S2 and S4 segments of the Shaker K+ channel. *Neuron* **16**, 1159–1167 (1996).
12. Larsson, H.P., Baker, O.S., Dhillon, D.S. & Isacoff, E.Y. Transmembrane movement of the Shaker K+ channel S4. *Neuron* **16**, 387–397 (1996).
13. Starace, D.M., Stefani, E. & Bezanilla, F. Voltage-dependent proton transport by the voltage sensor of the Shaker K+ channel. *Neuron* **19**, 1319–1327 (1997).
14. Yellen, G. The moving parts of voltage-gated ion channels. *Q. Rev. Biophys*. **31**, 239–295 (1998).
15. Bezanilla, F. The voltage sensor in voltage-dependent ion channels. *Physiol. Rev*. **80**, 555–592 (2000).
16. Starace, D.M. & Bezanilla, F. Histidine scanning mutagenesis of basic residues of the S4 segment of the Shaker K^+ channel. *J. Gen. Physiol.* **117**, 469–490 (2001).
17. Santoro, B. et al. Identification of a gene encoding a hyperpolarization- activated pacemaker channel of brain. *Cell* **93**, 717–729 (1998).
18. Ludwig, A. et al. Two pacemaker channels from human heart with profoundly different activation kinetics. *EMBO J.* **18**, 2323–2329 (1999).
19. Seifert, R. et al. Molecular characterization of a slowly gating human hyperpolarization-activated channel predominantly expressed in thalamus, heart, and testis. *Proc. Natl. Acad. Sci. USA* **96**, 9391–9396 (1999).
20. Anderson, J.A., Huprikar, S.S., Kochian, L.V., Lucas, W.J. & Gaber, R.F. Functional expression of a probable *Arabidopsis thaliana* potassium channel in *Saccharomyces cerevisiae*. *Proc. Natl. Acad. Sci. USA* **89**, 3736–3740 (1992).
21. Zei, P.C. & Aldrich, R.W. Voltage-dependent gating of single wild-type and S4 mutant KAT1 inward rectifier potassium channels. *J. Gen. Physiol.* **112**, 679–713 (1998).
22. Chen, J., Mitcheson, J.S., Lin, M. & Sanguinetti, M.C. Functional roles of charged residues in the putative voltage sensor of the HCN2 pacemaker channel. *J.* Biol. Chem. **275**, 36465–36471 (2000).
23. Shin, K.S., Rothberg, B.S. & Yellen, G. Blocker state dependence and trapping in hyperpolarization-activated cation channels: evidence for an intracellular activation gate. *J. Gen. Physiol.* **117**, 91–101 (2001).
24. Rothberg, B.S., Shin, K.S., Phale, P.S. & Yellen, G. Voltage-controlled gating at the intracellular entrance to a hyperpolarization-activated cation channel. *J. Gen. Physiol.* **119**, 83–91 (2002).
25. Mannikko, R., Elinder, F. & Larsson, H.P. Voltage-sensing mechanism is conserved among ion channels gated by opposite voltages. *Nature* **419**, 837–841 (2002).
26. Schlosser, A., Meldorf, M., Stumpe, S., Bakker, E.P. & Epstein, W. TrkH and its homolog, TrkG, determine the specificity and kinetics of cation transport by the Trk system of *Escherichia coli. J. Bacteriol.* **177**, 1908–1910 (1995).
27. Ahmed, A. et al. A molecular target for viral killer toxin: TOK1 potassium channels. *Cell* **99**, 283–291 (1999).
28. Sesti, F., Shih, T.M., Nikolaeva, N. & Goldstein, S.A. Immunity to K1 killer toxin: internal TOK1 blockade. *Cell* **105**, 637–644 (2001).
29. Ketchum, K.A., Joiner, W.J., Sellers, A.J., Kaczmarek, L.K. & Goldstein, S.A.N. A new family of outwardly-rectifying potassium channel proteins with two pore domains in tandem. *Nature* **376**, 690–695 (1995).
30. Saimi, Y., Loukin, S.H., Zhou, X.L., Martinac, B. & Kung, C. Ion channels in microbes. Methods Enzymol. **294**, 507–524 (1999).
31. Zerangue, N., Schwappach, B., Jan, Y.N. & Jan, L.Y. A new ER trafficking signal regulates the subunit stoichiometry of plasma membrane K(ATP) channels. *Neuron* **22**, 537–548 (1999).
32. Chen, G.Q., Cui, C., Mayer, M.L. & Gouaux, E. Functional characterization of a

potassium-selective prokaryotic glutamate receptor. *Nature* **402**, 817–821 (1999).
33. Spector, P.S., Curran, M.E., Zou, A., Keating, M.T. & Sanguinetti, M.C. Fast inactivation causes rectification of the IKr channel. *J. Gen. Physiol.* **107**, 611–619 (1996).
34. Smith, P.L., Baukrowitz, T. & Yellen, G. The inward rectification mechanism of the HERG cardiac potassium channel. *Nature* **379**, 833–836 (1996).
35. Chen, S., Wang, J. & Siegelbaum, S.A. Properties of hyperpolarization- activated pacemaker current defined by coassembly of HCN1 and HCN2 subunits and basal modulation by cyclic nucleotide. *J. Gen. Physiol*. **117**, 491–504 (2001).
36. Kaupp, U.B. & Seifert, R. Molecular diversity of pacemaker ion channels. *Annu. Rev. Physiol.* **63**, 235–257 (2001).
37. DiFrancesco, D. Characterization of single pacemaker channels in cardiac sino-atrial node cells. *Nature* **324**, 470–473 (1986).
38. Hoshi, T. Regulation of voltage dependence of the KAT1 channel by intracellular factors. *J. Gen. Physiol.* **105**, 309–328 (1995).
39. Hoth, S. Distinct molecular bases for pH sensitivity of the guard cell K^+ channels KST1 and KAT1. *J. Biol. Chem.* **274**, 11599–11603 (1999).
40. del Camino, D., Holmgren, M., Liu, Y. & Yellen, G. Blocker protection in the pore of a voltage-gated K+ channel and its structural implications. Nature 403, 321–325 (2000).
41. Zheng, J. & Sigworth, F.J. Selectivity changes during activation of mutant Shaker potassium channels. *J. Gen. Physiol.* **110**, 101–117 (1997).
42. Kiss, L. & Korn, S.J. Modulation of C-type inactivation by K^+ at the potassium channel selectivity filter. *Biophys. J.* **74**, 1840–1849 (1998).
43. Loots, E. & Isacoff, E.Y. Protein rearrangements underlying slow inactivation of the Shaker K+ channel. *J. Gen. Physiol.* **112**, 377–389 (1998).
44. Kiss, L., LoTurco, J. & Korn, S.J. Contribution of the selectivity filter to inactivation in potassium channels. *Biophys. J*. **76**, 253–263 (1999).
45. Liu, J. & Siegelbaum, S.A. Change of pore helix conformational state upon opening of cyclic nucleotide-gated channels. *Neuron* **28**, 899–909 (2000).
46. Flynn, G.E. & Zagotta, W.N. Conformational changes in S6 coupled to the opening of cyclic nucleotide-gated channels. *Neuron* **30**, 689–698 (2001).
47. Zilberberg, N., Ilan, N. & Goldstein, S.A. KCNKO: opening and closing the 2- P-domain potassium leak channel entails 'C-type' gating of the outer pore. *Neuron* **32**, 635–648 (2001).
48. Ko, C.H. & Gaber, R.F. TRK1 and TRK2 encode structurally related K^+ transporters in *Saccharomyces cerevisiae*. *Mol. Cell. Biol*. **11**, 4266–4273 (1991).
49. Goldstein, S.A.N., Price, L.A., Rosenthal, D.N. & Pausch, M.H. ORK1, a potassium-selective leak channel with two pore domains cloned from *Drosophila melanogaster* by expression in *Saccharomyces cerevisiae*. *Proc. Natl. Acad. Sci. USA* **93**, 13256–13261 (1996).
50. Gustin, M.C., Zhou, X.L., Martinac, B. & Kung, C. A mechanosensitive ion channel in the yeast plasma membrane. *Science* **242**, 762–765 (1988).